# Characterization of Starburst Dendrimers by EPR. 3. Aggregational Processes of a **Positively Charged Nitroxide Surfactant**

# M. Francesca Ottaviani\*

Department of Chemistry, University of Florence, 50121 Florence, Italy

# Nicholas J. Turro and Steffen Jockusch

Department of Chemistry, Columbia University, New York, New York 10027

### Donald A. Tomalia

Michigan Molecular Institute, Midland, Michigan 48640

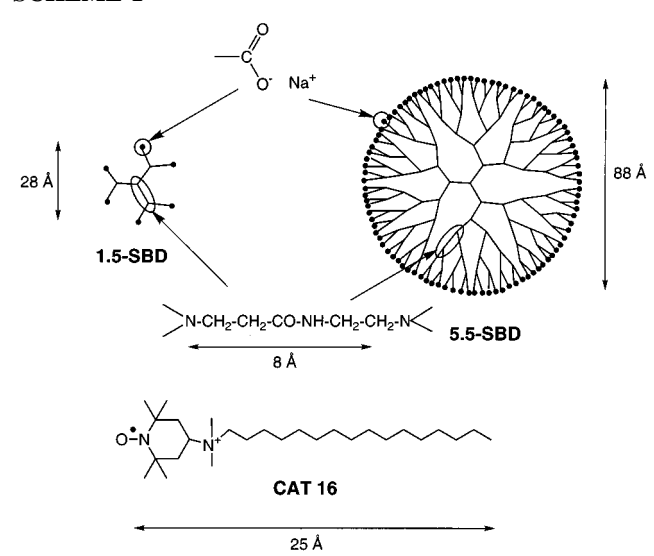
Received: January 29, 1996; In Final Form: April 30, 1996<sup>⊗</sup>

The aggregation characteristics of aqueous solutions of a positively charged nitroxide surfactant (CAT16) in the presence and absence of half-generation polyamidoamine starburst dendrimers (n.5-SBDs) have been investigated by electron paramagnetic resonance (EPR). Computer simulation of the EPR spectra allowed the convenient extraction of several parameters that were related to the supramolecular structure of the aggregates formed by CAT16 and SBDs. From examination of the EPR spectra as a function of variation of the concentration of CAT16, the concentration of SBDs, and the ionic strength and application of the EPR parameters available from simulation of the spectra, a paradigm for the structure and dynamics of the aggregates formed by CAT16 in the presence and absence of SBDs under various conditions is deduced. A study of the fluorescence quenching of pyrene in the presence of CAT16 is compared to a previous investigation of the interaction of SBDs with cationic surfactants. It is concluded that at low SBD concentration, for earlier generation SBDs ( $G \le 3.5$ ), whose size is smaller than or comparable to the size of the CAT16 micellar aggregates, the SBDs act as "guests" that bind to the micelles that serve as "hosts". In contrast, at low SBD concentration of the later generation SBD (G > 3.5), the size of the SBD is now larger than that of the micelles so that the latter can serve as "guests" for the former. A bilayer aggregate of the surfactant on the SBD is proposed. Finally, at high concentration of the later generation SBD, it is proposed that because of the large number of sites compared to the number of surfactants, an aggregate in which two or more SBDs are bridged by bilayers is formed by the surfactant and coexists with CAT16 micelles.

# Introduction

Cascade (dendritic) polymers are a novel class of macromolecules possessing branched, repeating units emanating from a central core. The controlled synthesis of dendrimers produces structures with nanoscopic size and well-defined composition and constitution.<sup>1-3</sup> The polyamidoamine family of starburst dendrimers (SBDs) is synthesized by grafting the repeating layers of amidoamine units starting from an ammonia core.1 Each shell of the amidoamine units constitutes a "full" generation (G) terminating with an external shell of amino groups. This family of starburst dendrimers possesses a certain similarity to biomacromolecules such as proteins and enzymes. Molecular simulation<sup>4</sup> of the SBD structure (in this paper SBD will always refer to polyamidoamine dendrimers) has revealed a rather dramatic change in the dendrimer morphology occurring after the full third generation. The so-called earlier generation dendrimers (G < 3) were found to possess an asymmetric shape and open structure, whereas the later generation dendrimers (G > 3) possess a nearly spherical shape and a densely packed external structure. Branches at the external surface of the SBDs may be terminated at half-generation (G = n.5) by forming carboxylate groups with sodium contraions (Scheme 1 shows a schematic of representative earlier and later generation n.5-SBD structure). The external structure and shape of these n.5-SBDs also bear a formal resemblance to anionic micelles. Therefore,

# **SCHEME 1**



the n.5-SBDs may be good models for both biomacromolecular and micellar structures.

Photophysical studies have been carried out to support the conclusion of molecular simulation that the dendrimer morphology varies qualitatively from earlier to later generations,5 and this conclusion has tested the similarities between n.5-SBDs and anionic micelles.<sup>6</sup> Analysis of electron paramagnetic

<sup>&</sup>lt;sup>®</sup> Abstract published in Advance ACS Abstracts, July 1, 1996.

resonance (EPR) spectra of paramagnetic probes has provided insight into the characterization of water solutions of *n*.5-SBDs.<sup>7,8</sup> For example, identification and structural characterization by means of EPR of the complexes formed by Cu<sup>II</sup> with internal and external ligand groups in the *n*.5-SBD structure have demonstrated that the SBDs show binding abilities with metal contraions that are very similar to biomacromolecules such as proteins.<sup>7</sup>

In a recent report from this research group, 8 positively charged nitroxide radicals possessing carbon chains of different lengths have been used as probes to investigate the interacting abilities of hydrophilic and hydrophobic ligand-binding sites in the n.5-SBD structure. A primary, noncooperative interaction of these radicals was proposed to be due mainly to electrostatic interactions between the positively charged nitroxide groups and the negatively charged n.5-SBD surface. However, evidence was also found to support the conclusion that the radical chain may partially penetrate the SBD surface and interact with hydrophobic sites near the SBD/water interface. Long chain nitroxides also behave as surfactants and, therefore, tend to aggregate in aqueous solution. In the previous report, 8 the concentration of the radical surfactants was mantained well below the critical micellar concentration (cmc) to avoid self-aggregation of the surfactants themselves in order to study only primary, noncooperative interactions with n.5-SBDs.

The present study involves a long chain nitroxide, 4-(N,Ndimethyl-N-hexadecylammonium)-2,2,6,6-tetramethylpiperidine-N-oxyl iodide (CAT16), both below and above the cmc, in order to investigate the aggregational behavior of this surfactant in the absence and in the presence of n.5-SBDs. Scheme 1 shows the formula of CAT16 and a two-dimensional projection of 1.5and 5.5-SBDs that were the main SBDs employed in the present report as typical of earlier and later generations SBDs. [We note that the nomenclature of the SBD generation has recently been changed<sup>8</sup> and the nomenclature in this paper conforms to this change. In the new nomenclature one unit is added to the old generation number, i.e., n.5-SBD (new) = 1 + n.5-SBD (old)]. Long chain nitroxide radicals have already been shown by means of EPR spectral analysis to monitor the formation of their own micelles and the micelles formed by other surfactants. 9-16 In this report, computer-aided analysis of the EPR spectra allowed monitoring the formation and the structural modification of CAT16 aggregates that form at the n.5-SBD/ water interface.

The solution interactions of macromolecules with ionic surfactant molecules are of fundamental relevance to industrial and biological processes.<sup>17-22</sup> For instance, the structure of biological membranes, the transport of material within biological systems, and several petrochemical and pharmaceutical industrial processes are based mainly on the interactions between natural or synthetic polyelectrolytes and surfactant aggregates in the form of micelles, vesicles, bilayers, and multilayers. These interactions and the complexes formed between polyelectrolytes and surfactant aggregates have been the subject of a range of investigations in recent years. 17-22 In particular, the aggregation of dodecyl trimethylammonium bromide (DTAB) in n.5-SBD solutions has been investigated using the fluorescence probe method.<sup>17</sup> The latter investigation describes the formation of both primary (noncooperative) and secondary (cooperative) binding of DTAB at the SBD/water interface as a function of DTAB concentration and SBD generation. This study provided a reference point for comparison with the binding interactions and aggregation processes of the cationic surfactant CAT16 in the presence of different generation n.5-SBDs. In this report the fluorescence of pyrene has also been analyzed as a function of CAT16 concentration in the absence and in the presence of n.5-SBDs. In addition, the aggregational behavior of CAT16 molecules in the absence of n.5-SBDs was investigated by both surface tension and EPR measurements. The results are interpreted in terms of supramolecular structures formed by the interaction of CAT16 monomers and aggregates ("perturbed micelles") with SBDs.

### **Experimental Section**

All the aqueous solutions used in this work were obtained by using doubly distilled water filtered through Millipore filters.

The polyamidoamine family of SBDs employed in this study has been synthesized as described in previous papers.<sup>1</sup> Methylester-terminated generations were hydrolyzed with stoichiometric amounts of NaOH in methanol to obtain sodium carboxylate external groups with sodium gegenions. The *n*.5-SBDs were purified from water solutions that were prepared and stored under nitrogen at ca. 278 K.

Sodium chloride (Merck), sodium acetate (Merck), and CAT16 (Molecular Probes) were used as received. Water solutions of CAT16 were prepared at a concentration of 2 mM and diluted as necessary. CAT16 micellar solutions possess a Kraft point of 313 K.<sup>23</sup> However, EPR analysis (*vide infra*) showed that the solubilization of CAT16 micelles was more conveniently achieved at 333 K. Therefore, all solutions of CAT16, with and without *n*.5-SBDs, were prepared and stored at 333 K. Since aging of the samples stored at 333 K showed a progressive decrease in the EPR signal intensity, presumably due to a thermal degradation process, freshly prepared CAT16 solutions were used for all the EPR measurements that were performed at 333 K.

Pyrene (Aldrich 99%) was recrystallized from ethanol. Water-saturated solutions of pyrene were used for all the fluorescence measurements.

EPR spectra were recorded by means of a Bruker 200D spectrometer operating in the X band, interfaced with Stelar software to an IBM-PC computer for data acquisition and handling. The temperature was controlled with the aid of a Bruker ST 100/700 variable-temperature assembly. Magnetic parameters were measured by field calibration with the 1,1-diphenyl-2-picryl hydrazine radical ( $g=2.00\,36$ ). Precision in the determinations of the correlation time for motion and of the spin exchange frequency was 5%, which was achieved from the fitting between the experimental and the computed EPR spectra. Precision in the determination of the hyperfine coupling constant,  $A_{\rm N}$ , was 0.05 G. Precision in the evaluation of the percentages of the spectral components was estimated to be ca. 2%.

Surface tension values were determined by using a DuNouy ring method with the aid of a Sigma70 KSV tensiometer.

Pyrene fluorescence spectra were recorded at 333 K for air-saturated samples with a SPEX Fluorolog spectrofluorometer.

# Results

**Example of Experimental and Simulated Spectra. Terminology.** Spectrum a in Figure 1 shows the EPR experimental spectrum recorded from a 2 mM aqueous solution of CAT16 (above the cmc). This spectrum (spectrum a) consists of signals assignable to two components superimposed on each other. (1) One component is a signal consisting of three narrow (ca. 1 G) lines arising from monomer nitroxide radicals that are free in solution. As expected, CAT16 solutions (0.2 mM) below the cmc showed only this three-line signal (spectrum b in Figure 1), which is termed f ("free" nitroxide monomer). (2) The other component is a signal consisting of a single broad (ca. 9 G)

line arising from nitroxide radicals that are aggregated in micelles. Because of their proximity in micellar aggregates, spin-spin interactions, predominantly Heisenberg exchange narrowing, cause a collapse of the three lines corresponding to the monomer into a single line.<sup>24–26</sup> This signal is expected and found to appear only above a critical concentration (cmc, vide infra) and is termed signal m ("micellized" nitroxides). The simultaneous observation of f and m in the experimental EPR spectrum requires that the CAT16 nitroxide radicals are distributed in two distinct environments, free solution and micellar aggregates, that are in slow exchange on the EPR time scale. The percentage of the micellar component m was obtained by subtraction of the signal f in the appropriate amount from the experimental spectrum.

Method for Simulation of Experimental Spectra. EPR and Molecular Parameters. The observed EPR spectra were simulated by means of the well-established procedure of Schneider and Freed.<sup>27</sup> The main input parameters used in the calculation of the spectra were the following.

(i) Principal Component of the g and  $A_N$  Tensors for the Zeeman (Electron Spin-Magnetic Field) and Hyperfine (Electron Spin-Nuclear Spin) Couplings. Spectrum c in Figure 1 shows the computed signal f arising from free CAT16 molecules in solution. For the computation of the observed spectra, the following magnetic parameters reported for the same type of radicals in a previous report<sup>16b</sup> were employed:

$$g_{xx} = 2.0088$$
  $A_{xx} = 6.8 \text{ G}$   
 $g_{yy} = 2.0072$   $A_{yy} = 8.2 \text{ G}$   
 $g_{zz} = 2.0035$   $A_{zz} = 35.7 \text{ G}$   
 $\langle g \rangle = 2.0065$   $\langle A_N \rangle = 16.9 \text{ G}$ 

However, the computed spectrum of CAT16 in micellar aggregates (signal m), which is shown in spectrum e, indicated a shift of the central field of the adsorption, which corresponded to the variation of the g value from 2.0065 to 2.0071.

We selected the following similar parameters reported<sup>16b</sup> for CAT12/perfluoropolyether (PFPE)-NH<sub>4</sub> mixed micelles, modified to account for the measured variation of g in the experimental signal:

$$g_{xx} = 2.0090$$
  $A_{xx} = 7.5 \text{ G}$   
 $g_{yy} = 2.0084$   $A_{yy} = 6.5 \text{ G}$   
 $g_{zz} = 2.0039$   $A_{zz} = 34.7 \text{ G}$   
 $\langle g \rangle = 2.0071$   $\langle A_N \rangle = 16.2 \text{ G}$ 

In comparison with the data for CAT16 in pure water solution, g increases, whereas  $A_N$  decreases. This decrease reflects a lower polarity of the environment sensed by the radical,<sup>28</sup> as expected if the probe were bound to a more hydrophobic micellar medium than a purely aqueous environment. A decrease of  $A_N$  has been reported for radical surfactants that insert into micellar aggregates.<sup>14</sup>

(ii) Principal Components of the Rotational Diffusion Tensor **D**. Rotational Correlation Time,  $\tau_c$ . A Brownian rotational diffusion motion was assumed to modulate the magnetic parameters. Therefore, the correlation time,  $\tau_c$ , is the time characteristic for the rotational diffusion and is related to the rotational diffusion coefficient, D, by the relationship  $\tau_c$  = 1/(6D). The following  $\tau_c$  values were used for the computation

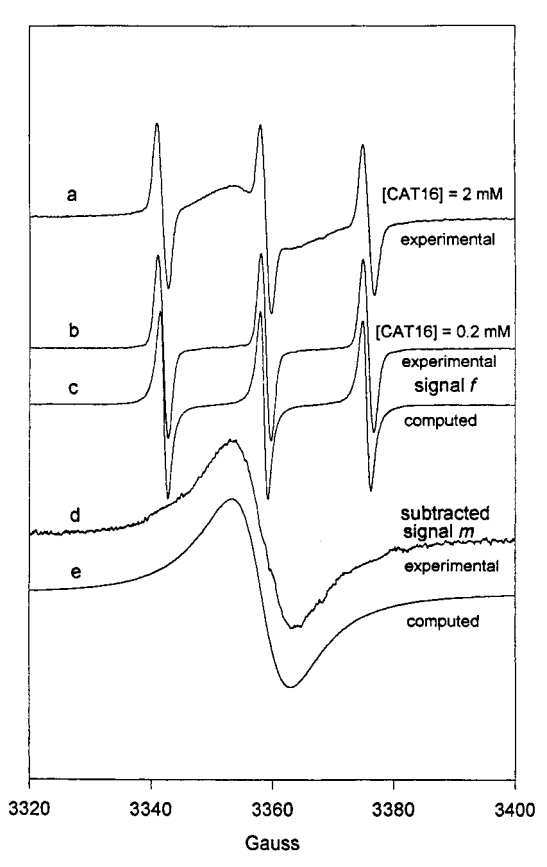


Figure 1. (a) EPR experimental spectrum of CAT16 in water (2 mM) at 333 K; (b) EPR experimental spectrum of CAT16 in water (0.2 mM) at 333 K; (c) computation of the experimental spectrum b = signal f; (d) EPR spectrum obtained by subtracting spectrum c from spectrum a; (e) computation of the subtracted component = signal m.

of the two signals f and m shown in Figure 1:

signal	spectrum in Figure 1	$\tau_{\rm c}$ (s)	
f	d	$4 \times 10^{-11}$	
m	c	$1 \times 10^{-9}$	

A value of  $\tau_c = 4 \times 10^{-11}$  s is a value characteristic for fast moving radicals in nonviscous homogeneous solution. The line shape of signal m is poorly affected by the variation of  $\tau_c$ . Furthermore, a single correlation time to describe the complex motion in the aggregates is an oversimplification. Therefore, the reported value of  $\tau_c$  simply indicated the decreased rotational mobility of the radical inserted in their own micelles. 14-16 The correlation time  $\tau_c$  for radical motion is generally associated with the rotational mobility of the radical around the Z axis (the direction of the  $p_7$  orbital on the nitrogen atom containing the unpaired electron), which should correspond to the main direction of the carbon chain attached to the radical group.

(iii) Heisenberg Spin Exchange Frequency,  $\omega_{ex}$ . Heisenberg spin exchange is a dynamic isotropic effect due to the collision of radicals at high local concentration.<sup>24</sup> An increase in the spin exchange frequency,  $\omega_{\rm ex}$ , therefore indicates an increase in the local concentration of radicals, i.e., micelle formation or formation of some other form of aggregates. For surfactant nitroxides forming aggregates,  $\omega_{ex}$  is a relevant parameter for the analysis of the EPR spectra, since it may be qualitatively correlated to the structure of the density of packing of the radicals in aggregates, i.e., the larger the value of  $\omega_{\rm ex}$ , the greater the density of packing. Spectrum c in Figure 1 was computed with  $\omega_{\rm ex} = 5.8 \times 10^8$  Hz, which is taken as typical for packing of the CAT16 molecules in its own micelles.

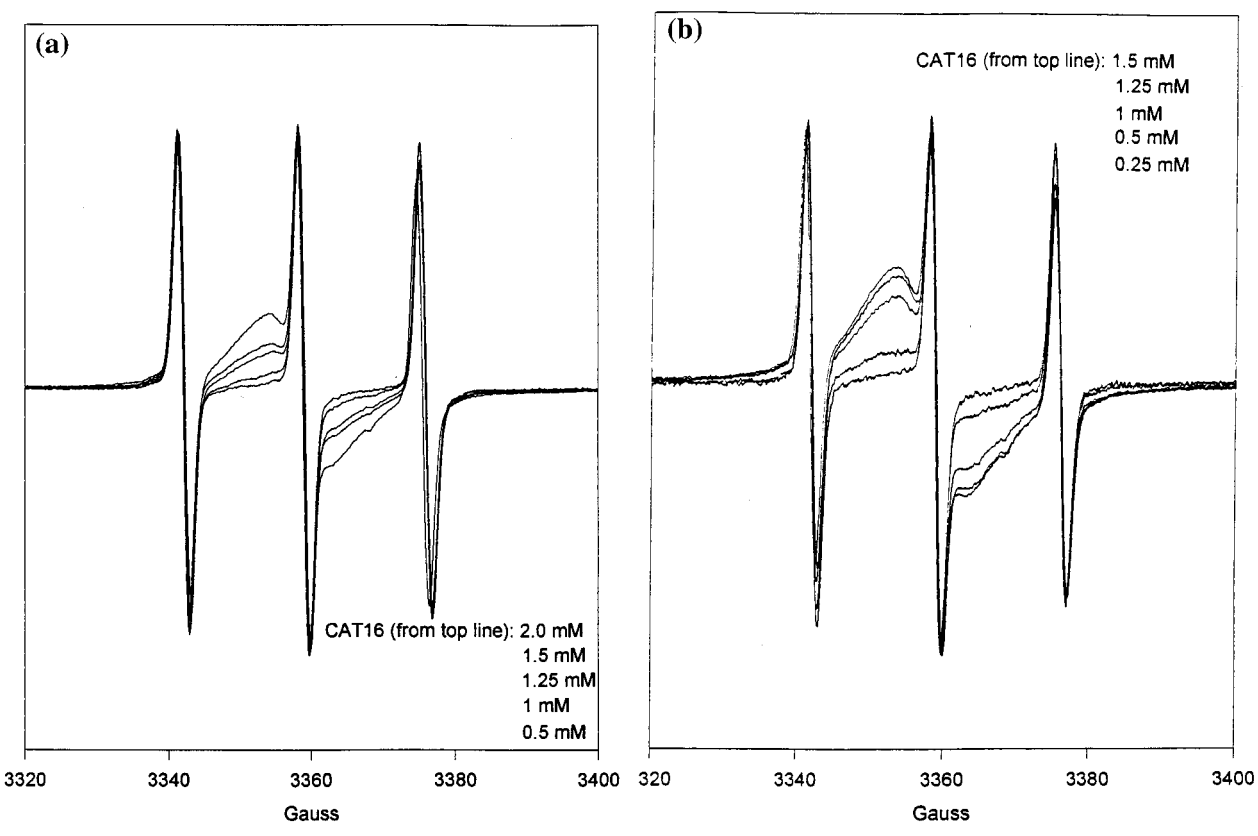


**Figure 2.** (a) EPR experimental spectra (333 K) of CAT16 solutions at different concentrations; (b) EPR experimental spectra (333 K) of CAT16 solutions at different concentrations in the presence of 1.5-SBD at concentration 0.2 M in carboxylate groups. The spectra are normalized at the height of the central peak of the three-line component (signal f).

(iv) Intrinsic Line Width  $1/T_{2,0}$ . The intrinsic line width  $1/T_{2,0}$  accounts for all inhomogeneous broadening arising from non-motional sources. The same  $1/T_{2,0}$  was used for computation of both spectra c and e, that is,  $1/T_{2,0} = 1.0$  G.

Computation of signals m and f as the appropriate components of the experimental line shape (spectrum a) was checked by combining the two computed components (spectra c and e) in appropriate amounts to obtain the best fit of the experimental line shape.

The combination of the spectra allowed the evaluation of magnetic and motional parameters of the two main components together with the partitioning of the radicals between the two environments, i.e., bulk solution and micellar aggregates. This procedure was also followed to evaluate parameters and percentages of the components constituting the EPR spectra in the presence of n.5-SBDs ( $vide\ infra$ ).

**Evaluation of the cmc of CAT 16**. The "classical" method of surface tension of CAT16 (I<sup>-</sup> salt) solutions was employed to evaluate the cmc of CAT16. The marked change in the slope of the surface tension (dyn/cm) vs —log[CAT16] occurring at [CAT16] = 0.25 mM ( $\pm 10\%$ ) is conventionally interpreted as the cmc of CAT16 in water solution (see Supporting Information). However, signal m due to the micelle formation was recognizable in the overall EPR signal at [CAT16] = 0.6 mM. The extrapolated CAT16 concentration at which signal m was recognizable in the spectra was evaluated as 0.4 mM  $\pm$  0.1 (see below) that was assumed to be the cmc by EPR.

Other measurements of the cmc of CAT16 by EPR<sup>29</sup> result in a value of cmc = 0.46 mM  $\pm$  0.05 for CAT16 (Br<sup>-</sup> salt). This value agrees well with the value obtained in our study, despite the different contraion (Br<sup>-</sup> instead of I<sup>-</sup>).

EPR Response to the Variation in CAT16 Concentration at Fixed Concentration of SBD Carboxylate Groups. Effects of Generation and Ionic Strength. The relative intensity of signal m at which this signal became detectable (at ca. 0.6 mM CAT16) in the overall line shape corresponded to more than 25-30% of CAT16 bound in the form of micelles. With a further increase in CAT16 concentration, the intensity of signal m increased directly with the decrease in the intensity of signal f. This is clearly shown in Figure 2a, which displays the EPR spectra of CAT16 at different concentrations, normalized at the height of the central peak of signal f. The effect of the addition of n.5-SBDs on the EPR spectra is given in Figure 2b, which shows the spectra of solutions of CAT16 at different concentrations in the presence of 1.5-SBD at a fixed concentration of 0.2 M in carboxylate groups. By comparing parts a and b of Figure 2, it is clear that the addition of the dendrimers led to an increase in the relative intensity of signal m (large concentration of aggregates). As described above, the relative intensity of signal m provided the percentage of CAT16 aggregates.

Analysis of Figure 2 demonstrates how the addition of n.5-SBDs provokes a shift of the cmc of CAT16 toward lower concentrations of the surfactant. This effect may be ascribed to some special characteristics of supramolecular aggregates formed by the binding of CAT16 to SBDs or to the influence of an increase in ionic strength, which is well-known to affect micellar size and shape and, consequently, the cmc. 30,31,14c To determine the relationship of ionic strength to the shift of cmc induced by the n.5-SBDs, EPR spectra were recorded for solutions of CAT16 containing different concentrations of the simple electrolytes, sodium acetate (NaOAc) or NaCl at concentration 0.2 M. These spectra were compared to those obtained with solutions of differently sized SBD ([SBD-COO<sup>-</sup>] = 0.2 M) at various concentrations of CAT16. The cmc and the maximum percentages of the aggregates (max %) were given in Table 1. The spectral analysis was consistent with the following remarks. (1) Both NaOAc and NaCl decreased the

TABLE 1: Critical Micellar Concentration (cmc) and Maximum Percentages of the Aggregates (max %) for CAT16 in Water without and with Presence of Salts (0.2 M) or n.0-SBD ([SBD-COO<sup>-</sup>] = 0.2 M) Determined by EPR

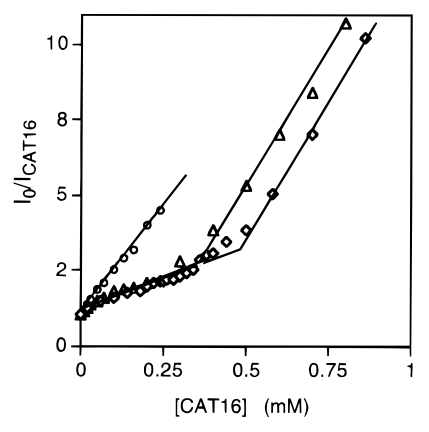
	NaCl	NaOAc	1.5-SBD	3.5-SBD	5.5-SBD	water
cmc (mM)	0.25	0.33	0.36	0.47	0.50	1.00
max %	87	84	83	77	74	75

cmc of CAT16 to a larger extent when compared to solutions containing 3.5-SBDs. NaCl was most effective in decreasing the cmc. (2) The line shapes of the two components, signals m and f, of the spectra of CAT16 micellar solutions were not modified by the addition of salts, i.e., the parameters evaluated from the spectra, like the correlation time for motion or the exchange frequency, were the same in the absence and in the presence of the salts. Conversely, the line shapes of signals m and f were modified by the addition of n.5-SBDs (vide infra). (3) The cmc is clearly different for CAT16 solutions containing different generation dendrimers. The difference cannot be ascribed solely to a variation in the ionic strength, since the three n.5-SBDs were used at constant concentration in ionic groups (COO<sup>-</sup> and Na<sup>+</sup>), i.e.,  $[SBD-COO^{-}] = 0.2 \text{ M}$ . We suggest that the cooperative interaction of CAT16 forms the supramolecular structures at the n.5-SBD/water interface.

Comparison of EPR Results with Fluorescence Probes of Cationic Surfactant-SBD Interactions. Formation of aggregates of a positively charged surfactant, DTAB, at the negatively charged surface of n.5-SBDs has been investigated by the pyrene fluorescence probe method<sup>17</sup> involving the measurements of the ratio of the third to the first vibrational band of pyrene monomer fluorescence,  $I_3/I_1$ . This probe parameter has been shown to be a reliable reporter of the environmental polarity sensed by pyrene.<sup>32</sup> The value of  $I_3/I_1$  = 0.63 has been reported for pyrene in water.<sup>33</sup> Larger values of  $I_3/I_1$  are associated with more hydrophobic (less polar) environments. For example, a value of  $I_3/I_1 = 1.2$  is found for pyrene in cetyltrimethylammonium chloride (CTAC) micelles,<sup>32</sup> consistent with the location of pyrene as a guest within the hydrophobic core or interface of the CTAC micelle.

We have employed pyrene as a fluorescence probe of CAT16 interactions with SBDs. Pyrene fluorescence was measured as a function of [CAT16] in the absence and in the presence of 1.5-, 2.5-, 4.5-, 6.5-, and 8.5-SBDs or in the presence of an equivalent amount (5 mM) of NaOAc. The ratio of the third to the first vibronic peaks did not change in the entire range of CAT16 concentration investigated. The value  $I_3/I_1 = 0.65$  was very close to the value reported<sup>33</sup> ( $I_3/I_1 = 0.63$ ) for pyrene in water. However, the intensity of the fluorescence signal decreased with the increase in CAT16 concentration, as expected from the quenching of pyrene fluorescence by the nitroxide moiety of the CAT16 radicals.

Figure 3 shows the Stern-Volmer plot of the ratio of the fluorescence intensities of pyrene, without and with the quencher CAT16, (I<sub>0</sub>/I<sub>CAT16</sub>), as a function of CAT16 concentration under three conditions: (1) for aqueous CAT16 solutions; (2) for aqueous solutions of CAT16 in the presence of n.5-SBDs at 5 mM in SBD-COO- groups; (3) for aqueous solutions of CAT16 in the presence of NaOAc at concentration 5 mM in  $COO^-$  groups (333 K). Interestingly, the  $I_o/I_{CAT16}$  variation as a function of [CAT16] for pure CAT16 solutions showed two different slopes. At [CAT16] < 0.4 mM, the pyrene fluorescence appears to be quenched dynamically by CAT16 with a rate constant  $k_q = 1.4 \times 10^{10} \text{ M}^{-1} \text{ s}^{-1} (\tau_0 = 175 \text{ ns}).^{33}$  This rate is typical of a diffusion-controlled equilibrium in aqueous solution, which is expected for CAT16 monomers in a pyrenesaturated solution at 333 K. At concentrations of CAT16 higher



- no additives
- n.5-SBD [COO<sup>-</sup>]=5mM
- NaOAc [COO]=5mM

Figure 3. Stern-Volmer plot of the ratio between the fluorescence intensities (fluorescence at 372 nm) of pyrene, without and with the quencher CAT16 (I<sub>o</sub>/I<sub>CAT16</sub>) as a function of CAT16 concentration for CAT16 pure solutions and for solutions of CAT16 in the presence of *n*.5-SBDs or NaOAc at concentration 5 mM in COO<sup>-</sup> groups:  $\lambda_{ex} =$ 333 nm; pyrene-saturated solutions.

than 0.4 mM, micelles were formed and the excited pyrene was quenched statically, corresponding to the second, steeper slope. Therefore, when micelles are formed, both static quenching and dynamic quenching occur. Since pyrene molecules are localized in the micellar aggregate, the excited pyrene trapped in the CAT16 micellar region was quenched statically by the nitroxide head groups of CAT16.

The cmc of CAT16 measured by the variation of the slope of the Stern-Volmer plot was higher (cmc by fluorescence is  $0.4~\mathrm{mM} \pm 10\%$ ) than the value obtained from surface tension measurements. However, the discrepancy between the two cmc measurements is ambiguous because of the low accuracy of the values (10%) and probably resides in different impurities influencing the cmc.

Addition of NaOAc perturbed the aggregation of CAT16. The Stern-Volmer plot showed a variation of slope at about [CAT16] = 0.3 mM, which should correspond to the cmc of the CAT16-pyrene system in the presence of NaOAc 5 mM. Therefore, the shift in cmc obtained by pyrene fluorescence quenching after addition of NaOAc was smaller than the shift measured by EPR. This effect is plausible because of the large NaOAc concentration used in the EPR experiments (0.2 M). Indeed, a 5 mM concentration of NaOAc in the CAT16 solutions provoked a very small shift in the cmc value measured by EPR (results not shown).

The results were quite different for the CAT16 solutions containing n.5-SBDs. The Stern-Volmer plot (Figure 3) shows a linear dependence on the concentration of CAT16 for [CAT16] below the cmc. However, the quenching slope is comparable to that observed for static quenching above the cmc, i.e., when CAT16 aggregates are present. Interestingly, different generation SBDs gave almost the same Stern-Volmer slopes. From the EPR results, the formation of CAT16 aggregates at the dendrimer/water interface took place below the cmc of pure CAT16 solutions. The excited pyrene is localized in the hydrophobic region of the aggregates that contain a high concentration of nitroxides, and therefore, an efficient static quenching occurred. However, the fluorescence-quenching measurements in the presence of the dendrimers showed both a strong variation of the cac (much larger than the cac variation measured by EPR) and a low sensitivity to generation (which

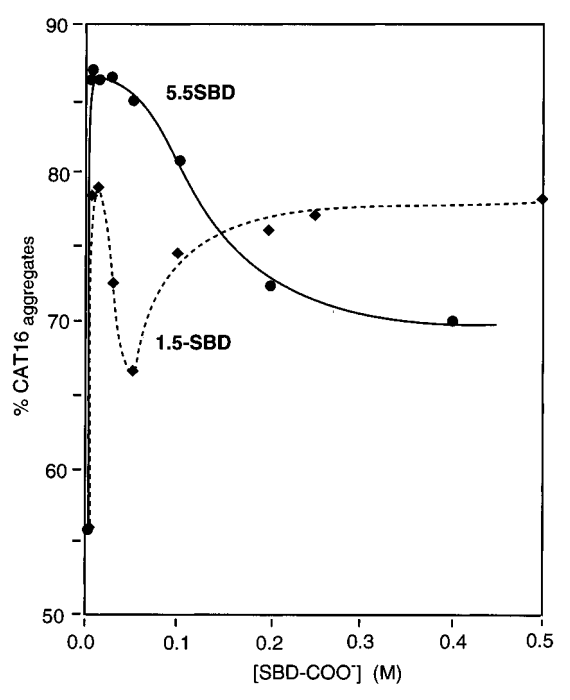


**Figure 4.** Variation of the percentage of CAT16 aggregates as a function of the concentrations of 1.5- and 5.5-SBD-COO<sup>-</sup> concentrations.  $\tau_c$  is evaluated by computation of the three-line component (signal f) of the experimental spectra at 333 K.

is in contrast with both the EPR results and the previous fluorescence results<sup>17</sup>).

EPR Response to the Variation in SBD Concentration at Fixed Concentration of CAT16 Carboxylate Groups. Effect of Generation. From the above results, it is clear that supramolecular aggregates are formed between CAT16 and SBDs and that both the dendrimer concentration and dendrimer generation are important parameters involved in determining the supramolecular structure of the CAT16-SBD aggregates formed under various ratios of CAT16/SBD. Therefore, to obtain pertinent experimental information on the structures of these supramolecular species, EPR spectra were recorded for samples at different SBD-COO- concentrations with a constant [CAT16]. From the analysis of these spectra the percentages of CAT16 aggregates were evaluated and are reported in Figure 4 as a function of the concentration of SBD-COO-.

Figure 4 shows the plot of the percentage of CAT16 aggregates as a function of the concentrations of 1.5- and 5.5-SBD-COO<sup>-</sup> at [CAT16] = 1.0 mM (above the cmc of CAT16). The dendrimer was therefore added in increasing amounts to a micellar solution of the surfactant. The salient features of the observed spectra are described below.

- (a) The fraction of aggregates at a [CAT16] = 1 mM (above the cmc) is ca. 55%. The addition of low concentrations of either earlier generation (1.5-SBD) or later generation (5.5-SBD) n.5, at ca. 0.01-0.02 M in [SBD-COO<sup>-</sup>], at first leads to a marked increase in CAT16 aggregates at the expense of the isolated monomers (Figure 4). The maximum increase was larger for the 5.5-SBD (87% aggregates) than for the 1.5-SBD (78% aggregates).
- (b) Even though the number of SBD-binding sites increases in this region, the tendency to form aggregates still increases until the maximum is reached for both 1.5-SBD and 5.5-SBD. The maximum corresponds roughly to a supramolecular stoichiometry of one surface group to one molecule of CAT16.
- (c) Although for both the 1.5-SBD and 5.5-SBD the fraction of aggregates reaches a maximum at ca. 0.02-0.03 M and then starts decreasing, the fraction of aggregates continues to decrease

with [SBD-COO<sup>-</sup>] for the addition of 5.5-SBD, but not for the 1.5-SBD, which reaches a minimum at ca. 0.05 M [SBD-COO<sup>-</sup>]. Evidently, the stoichiometry of the supramolecular structures involved in aggregate formation changes with respect to the number of SBD molecules involved.

It is noteworthy that, at [SBD-COO<sup>-</sup>] greater than 0.15 M, the fraction of CAT16 aggregates becomes larger for 1.5-SBD than for 5.5-SBD. Therefore, at the concentration of SBDs used for the measurements reported in Table 1 ([SBD-COO<sup>-</sup>] = 0.2 M), the relative intensity of signal m was higher for 1.5-SBD with respect to 5.5-SBD. At lower 5.5-SBD-COO<sup>-</sup> concentrations, the formation of aggregates at the SBD/water interface was favored even at the CAT16 concentrations below the cmc, which is well in line with the results obtained by fluorescence-quenching measurements (Figure 3).

Hyperfine Coupling Constants. Polarity of CAT16 Aggregates. As described above, analysis of the spectra allowed an evaluation of the parameters for each of the two components constituting the spectra, i.e., signals m and f. The main parameters evaluated from the computation of signal f were the hyperfine coupling constants,  $A_N$ , and the correlation times for motion,  $\tau_c$ . The coupling constants underwent a very small change in the various experimental conditions. Indeed, a more detailed analysis to Figure 2 showed that the peak to peak distance among the three hyperfine lines weakly decreased with the increase in CAT16 concentration, mainly by addition of n.5-SBDs. This decrease was more evident at the later generations. The following values for  $A_N$  of signal f were taken as representative:

system	$A_N(\mathbf{G})$
[CAT16] = 0.2  mM - no SBDs	16.9
[CAT16] = 1.0  mM - no SBDs	16.8
[CAT16] = 0.2  mM - 1.5-SBD	16.8
[CAT16] = 1.0  mM - 1.5-SBD	16.6
[CAT16] = 0.2  mM - 5.5-SBD	16.7
[CAT16] = 1.0  mM - 5.5-SBD	16.5

The variation of  $A_N$  is connected to a variation of the environmental polarity of the nitroxide group. Therefore, the decrease in  $A_N$  for CAT16 monomers in the presence of the dendrimers arose from a lower polarity around the CAT group. The monomers might undergo fast exchange among different environments: the bulk water solution, CAT16 aggregates, and the SBD/water interface. The polarity of these environments follows the trend SBD/water interface > bulk water solution > CAT16 aggregates. Consequently, we suppose that the lower the hyperfine constant, the longer the time the radicals spend in the vicinity of the CAT16 aggregates.

**Correlation Times of CAT16 Aggregates.** Simulation of signal f allows evaluation of the correlation times,  $\tau_c$ , for motion of CAT16 "free" monomers ([CAT16] = 1.0 mM, above the cmc) as a function of 1.5- and 5.5-SBD—COO $^-$  concentrations (Figure 5). For the addition of very small amounts (<0.05M) of 5.5-SBD, the value of  $\tau_c$  decreased, indicating that the mobility of the "isolated" monomers increased; the value of  $\tau_c$  reached a minimum. In contrast, the 1.5-SBD showed only an increase in  $\tau_c$  at concentrations below 0.05 M. However, above ca. 0.05 M the value of  $\tau_c$  increases relatively sharply for 5.5-SBD, whereas for 1.5-SBD only a relatively slight increase occurs for  $\tau_c$  with increasing [SBD—COO $^-$ ].

Electron Spin Exchange of the CAT16 Aggregates. Simulation of signal m allowed for evaluation of the exchange frequency for the Heisenberg spin—spin interactions, which is related to the molar fraction X, in their own micelles:  $^{34}$   $\omega_{\rm ex} = k'_{\rm ex} X$ , where  $k'_{\rm ex}$  is the proportionality constant. The variation of  $\omega_{\rm ex}$  may be, therefore, considered as a measure of the local

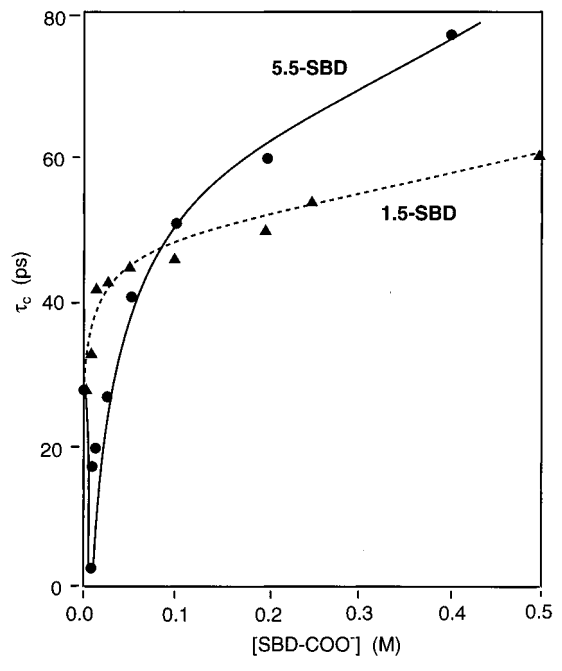


**Figure 5.** Correlation times for the diffusional rotational motion,  $\tau_c$ (s) for CAT16 solutions (1.0 mM) as a function of 1.5- and 5.5-SBD- $COO^-$  concentrations.  $\tau_c$  is evaluated by computation of the three-line component (signal f) of the experimental spectra at 333 K.

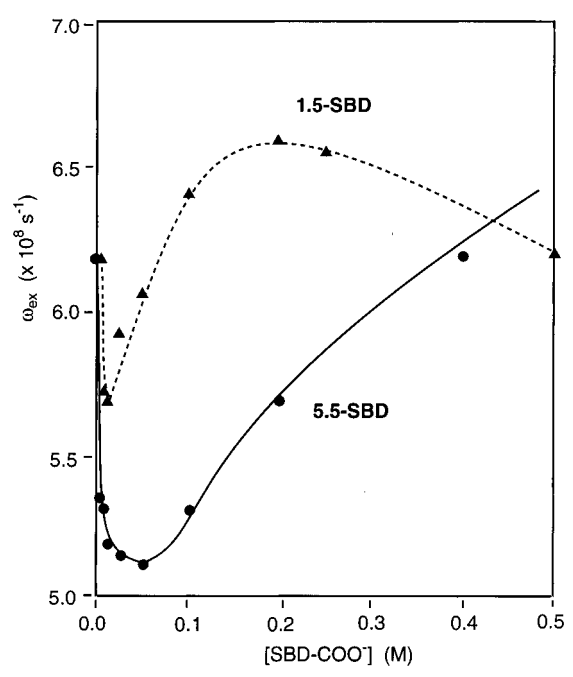


**Figure 6.** Plot of the Heisenberg spin-spin exchange frequency,  $\omega_{\rm ex}$  $(s^{-1})$  vs [SBD-COO<sup>-</sup>] for 1.5- and 5.5-SBDs at [CAT16] = 1 mM.

concentration of the radicals or the density of packing of the monomers in the aggregates.

Figure 6 exhibits the values of  $\omega_{\rm ex}$  as a function of [SBD-COO<sup>-</sup>]. It is noteworthy that for both the 1.5-SBD and the 5.5-SBD, the value of  $\omega_{\rm ex}$  experiences a minimum at [SBD- $COO^{-}$ ] < 0.1 M. The minimum for the 1.5-SBD is in the same region as for the maximum percentage aggregates (Figure 4).

# Discussion

Supramolecular Interpretation of the Results. Guest-Host Complexes of Surfactants and Starburst Dendrimers. We seek a supramolecular interpretation<sup>35</sup> of the EPR results observed for the SBD/CAT16 systems (above and below its cmc) in the presence and absence of earlier and later generation SBDs with 1.5-SBD and 5.5-SBD, respectively, serving as typical examples.

For CAT16 in the absence of SBD and below the cmc, the only pertinent structure (Scheme 2) is the CAT16 monomeric surfactant, 1. In the presence of SBD below the cmc, we postulate that the pertinent structures<sup>8,17</sup> are two supramolecular complexes 3, one representative of earlier generations (e.g., 1.5-SBD) and a second representative of later generations (e.g., 5.5-SBD).

Structure of CAT16 Aggregates above the cmc and in the Absence of SBD. In the absence of SBD above the cmc of CAT16, the two structures pertinent to the ESR spectra are the CAT16 free monomers (Scheme 2, 1) and the CAT16 monomers aggregated in micelles (Scheme 2, 2), both of which coexist in an equilibrium that is dynamic but slow on the EPR time scale. The values of the EPR parameters for the correlation time of the monomer,  $\tau_c$  (ca. 27 ps), for the polarity of the monomers,  $A_N$  (ca. 16.9 G), and for the packing of the micelle,  $\omega_{\rm ex}$ , were all relatively insensitive to CAT16 concentration above the cmc. For instance, a value of  $\omega_{\rm ex} = 5.8 \times 10^8 \, {\rm s}^{-1}$  was obtained for CAT16 in micellar solutions at [CAT16] = 2 mM, whereas at [CAT16] = 1 mM (Figure 6) a value of  $\omega_{\rm ex} = 6.2 \times 10^8 \, {\rm s}^{-1}$ was obtained.

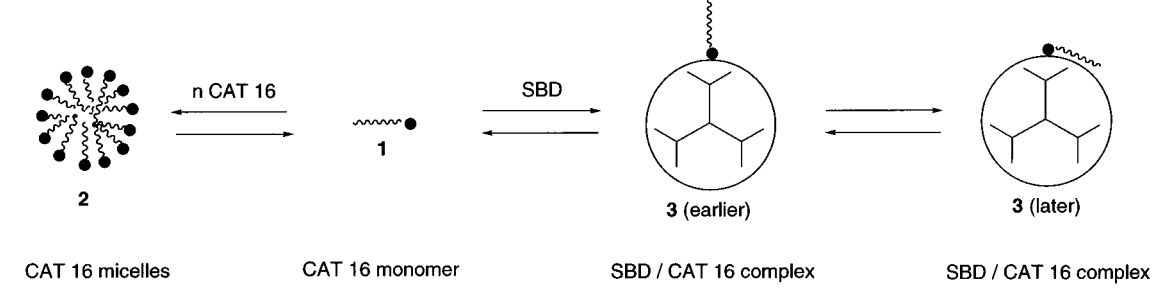
Although the cmc was shifted toward lower values by adding electrolytes such as NaOAc and NaCl, the values of the EPR parameters did not change significantly upon addition of electrolytes. These results are all consistent with the maintenance of the equilibrium between 1 and 2 and the existence of a similar micellar structure in the presence of electrolytes, are expected based on previous literature reports, 14 and provide confidence that the results in the presence of SBD are valid and can be plausibly interpreted in terms of the supramolecular structures in Schemes 2 and 3.

Micellar Aggregates in the Presence of SBD. It is clear from Figure 3 that addition of SBD leads to a higher fraction of signal m at a given [CAT16].

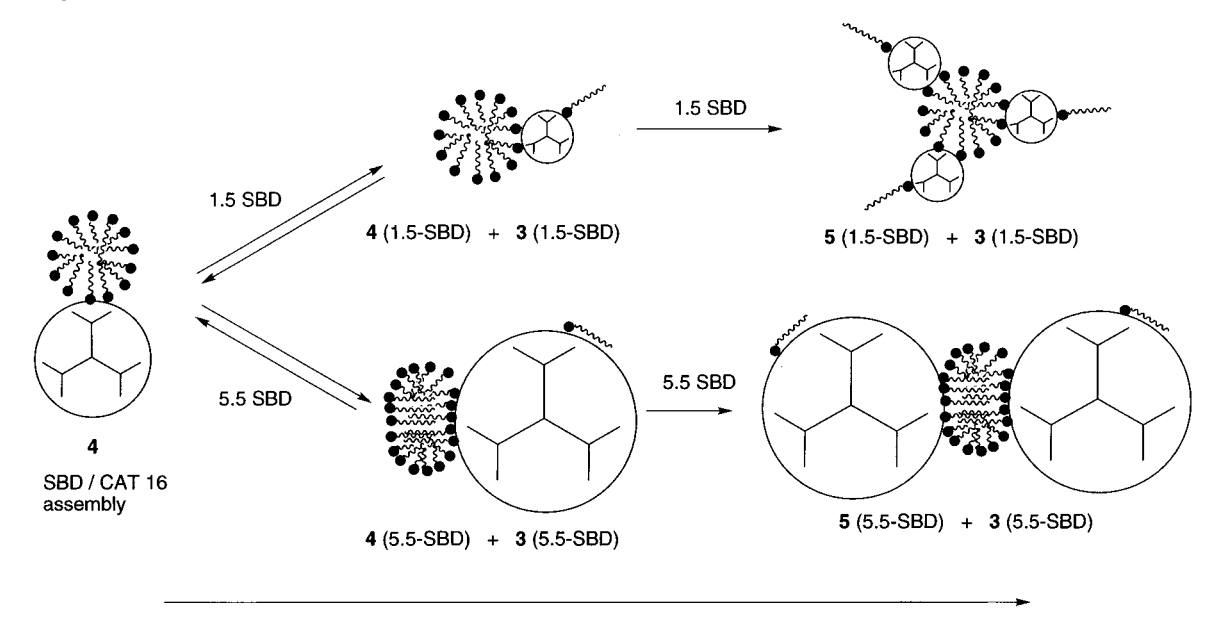
There are some well-established precedents for the formation of surfactant aggregates upon addition of a polyion to a solution of surfactant:  $^{14c,30,31}$  (1) the polyion increases the ionic strength of the solution, reducing the repulsions of the head groups in the micelles and thereby reducing the free energy for formation of surfactant micelles; (2) the polyion causes aggregation of the surfactant by "condensation" of the surfactant and the highly concentrated surface of the polyion domain and thereby causes the formation of surfactant aggregates on the surface of the polyion. The data in Table 1 clearly demonstrate that an increase in ionic strength resulting from addition of salts such as NaCl and NaOAc enhances the formation of CAT16 micelles. Thus, ionic strength is certainly an important factor in the formation of aggregates when the concentration of SBD is increasd, since the number of anionic surface groups and cationic counterion increases as [SBD-COO-] increases.

The data in Table 1 argue that in the presence of SBD, signal m should be assigned to an aggregate of CAT16 and SBD rather than to micelles of CAT16 alone. From inspection of the comparative fraction of m for the 1.5-SBD, 3.5-SBD, and 5.5-SBD (Table 1) it is clear that at fixed [SBD-COO<sup>-</sup>] the lower the SBD generation, the more effective the aggregation of CAT16 (1.5-SBD > 3.5-SBD > 5.5-SBD). Because the concentration of ionized groups is constant, the ionic strengths of the samples should be quite comparable, so we conclude that an effect beyond that of ionic strength must be operating and that the SBD and CAT16 interact in a manner that induces

#### **SCHEME 2**



#### **SCHEME 3**



[SBD] increase

[CAT 16] fixed above cmc

cooperative aggregation of CAT16, with the earlier generation being more effective in inducing aggregation than the later generation.

Supramolecular Structural Interpretation of the Formation of Aggregates as a Function of [SBD]. The data considered so far allow the conclusion that the aggregates being monitored by EPR are indeed supramolecular assemblies of both CAT16 and SBD such as those shown in Schemes 2 and 3. Moreover, the results presented in Figures 4-6 suggest that the supramolecular structures of the CAT16/SBD assemblies are different for the earlier (1.5-SBD) and later (5.5-SBD) generations. We can now interpret the features of the EPR results of Figures 4–6 in terms of the structures and equilibria of Schemes 2 and 3. Supramolecular structures are often considered within the framework of the noncovalent binding host/guest metaphor derived from enzyme chemistry.<sup>35</sup> Typically, the host possesses a greater size and a greater number of binding sites than the guest and serves to "template" the structure of aggregates of guest molecules. The size of CAT16 micelles (assuming a spherical model of diameter ca. 50 Å, the extended length of a surfactant chain) is larger than the relatively small size of the earlier generation 1.5-SBD (diameter ca. 28 Å from size exclusion chromatography). Thus, for structures such as 4 (1.5-SBD), the CAT16 micelle may be considered the host and the 1.5-SBD a bound guest. On the other hand, the size of CAT16 micelles is smaller than that of the later generation 5.5-SBD (diameter ca. 90 Å from size exclusion chromatography). Thus, for structures such as 4 (5.5-SBD), the SBD may be considered the host and the CAT16 monomers or a CAT16-perturbed micelle as bound guests. From these considerations it is plausible that the supramolecular structures (host/guest relationships) formed from CAT16/SBD are fundamentally different depending on whether the SBD is an "earlier" or a "later" generation. For CAT16 aggregates and SBDs at comparable size, we expect an intermediate behavior between those reported for the earlier and later generations, respectively.

Structures Present at Low Concentration (<0.05 M SBD-COO<sup>-</sup>) of Earlier and Later SBD. Upon addition of small amounts of SBD (ca. 0.02 M) the percent of aggregates increases to a maximum that is higher for 5.5-SBD than for 1.5-SBD. On this basis, we postulate that in the case of the CAT16/1.5-SBD systems, at low [SBD-COO-] the structure of the supramolecular assembly is determined by a micelle (host) that absorbs a single SBD (guest) molecule (Scheme 3, 4 (1.5-SBD)). Conversely, in the case of the CAT16/5.5-SBD, the SBD molecule acts as a host that absorbs the micelle (guest) (Scheme 3, 4 (5.5-SBD)). We assume that the aggregate portion of the supramolecular structure is a "distorted micelle" roughly spherical for small distortions and increasingly "bilayer-like" in structure as the interactions with the dendrimer surface grow stronger. In addition, these aggregates are postulated to be in equilibrium with the noncooperatively bound CAT16/SBD complexes, 3. The reasons for the bilayer character are those conventionally proposed for the distortion of micellar shapes, i.e., factors that reduce repulsions between micellar head groups will tend to increase the aspect ratio of micellar structures. A more pronounced bilayer structure is reasonable for the 5.5-SBD because of the smaller curvature of the surface and the higher charge density of the larger dendrimer. As the [SBD] increases, the fraction of 4 (1.5-SBD) and 4 (5.5-SBD) increases until a point is reached where the number of available SBD—COO—binding sites is so large that the noncooperatively bound complexes 3 (presumably with more than one monomer per SBD) begin to form in increasing amounts and thereby reduce the fraction of CAT16 aggregates observed. It is noted that an increase in ionic strength resulting from an increasing concentration of SBD is expected to enhance the formation of CAT16 micelles, which is contrary to the observations for this concentration region and further supports the formation of CAT16/SBD complexes.

The second EPR parameter that probes aggregate structure is the rate of spin exchange,  $\omega_{\rm ex}$ . Starting from the value of  $\omega_{\rm ex}$  of 6.2  $\times$  10<sup>8</sup> s<sup>-1</sup> for CAT16 micelles, the value of  $\omega_{\rm ex}$ decreases for both 1.5-SBD and 5.5-SBD upon addition of low [SBD-COO<sup>-</sup>] (Figure 6). However, the decrease in  $\omega_{\rm ex}$  was more significant for 5.5-SBD, as was evident from the deeper minimum for 5.5-SBD of  $\omega_{\rm ex}$  at about [5.5-SBD-COO<sup>-</sup>] = 0.05 M. Thus, at low [SBD] the aggregates formed from the larger SBD were therefore less densely packed (smaller value of  $\omega_{\rm ex}$ ) than those for the 1.5-SBD at equivalent [SBD-COO<sup>-</sup>]. We conclude that 4 (1.5-SBD) and 4 (5.5-SBD), postulated to be formed at low [SBD-COO<sup>-</sup>], are less densely packed than the CAT16 micelle (no SBD in Figure 6). The denser binding of 4 (1.5-SBD) relative to 4 (5.5-SBD) is consistent with the idea that the structure that least perturbs the tighter micelle structure (e.g., 4 (1.5-SBD) should show the denser packing.

The  $\tau_c$  parameter monitors the binding to SBD of the monomers of CAT16 rather than CAT16 aggregates. From Figure 5 it is seen that at low [5.5-SBD]  $\tau_c$  reaches a minimum, which corresponds to a large increase of micellized surfactants at the expense of free monomers (Figure 4). Since the monomers are nearly all aggregated, they are therefore prevented from the interaction with the SBD surface and their mobility increases. Both 1.5-SBD and 5.5-SBD show a decrease in mobility for a further increase of [SBD-COO-]. The results are consistent with the proposed model of an equilibrium between noncooperative binding of monomers to SBD (3) and cooperative binding to form aggregates on the surfaces of the SBD (4).

It is noted that the variation of  $\tau_c$  was smaller for CAT16 monomers than that reported for CAT*n* monomers by increasing [SBD-COO<sup>-</sup>] in the absence of CAT*n* aggregates,<sup>8</sup> i.e., below the cmc.

The EPR polarity parameter,  $A_N$ , showed a small variation in the presence (16.5–16.6 G) and absence (16.8 G) of SBD. The trend implies the sensing of a less polar environment experienced by the CAT16 monomer in the presence of SBD, consistent with the proposed structure **3**.

In summary, an equilibrium between the pairs of supramolecular structures **3** (1.5-SBD) and **4** (1.5-SBD) and **3** (5.5-SBD) and **4** (5.5-SBD) is consistent with the EPR results for low [SBD-COO<sup>-</sup>].

Structures Present at High Concentration (>0.05 M SBD-COO<sup>-</sup>) of Earlier and Later SBD. We now consider the supramolecular structures formed as [SBD-COO<sup>-</sup>] increases above ca. 0.05 M. From Figure 4 it is seen that the fraction of CAT16 aggregates in solutions of 1.5-SBDs reaches a minimum at about ca. 0.05 M in COO<sup>-</sup> groups and then increases upon a further increase of SBD concentration, whereas in this region of COO<sup>-</sup> concentration the fraction of CAT16 aggregates continues to decrease monotonically for the 5.5-SBD.

The minimum in the pattern reported for 1.5 generation in Figure 4 may result from (i) the competition between the dilution of CAT16 at the SBD/water interface, due to a large available dendrimer external surface, and the tendency of CAT16 to undergo aggregation in order to avoid the effect of the increased ionic strength of the solution or (ii) a regime with an intermediate exchange rate between two different aggregate types. Indeed, the increase in the number of SBD molecules will introduce a driving force for formation of aggregates possessing a composition containing more than one SBD molecule. In the case of the small size of the earlier dendrimers, it is postulated to lead to the simultaneous interaction of more than one SBD (guest) with a CAT16 micelle (host) (Scheme 3, 5 (1.5-SBD)).

From Figure 4 we deduce a qualitatively different supramolecular structure for the CAT16/SBD assemblies for the later generation relative to the earlier generation, since the fraction of aggregates decreases as the [COO<sup>-</sup>] increases. Since the [CAT16] is fixed in this analysis, the structural changes are associated with the increasing number of SBD molecules and binding sites in the presence of a fixed number of CAT16 molecules. For the 5.5-SBD, it is proposed that a cluster of CAT16 monomers form a "bridge" between two SBDs. More will be said about the 5.5-SBD system below.

The results shown in Figure 6 (exchange frequencies) reveal that the packing of the CAT16/SBD aggregates increases for both the 1.5-SBD and the 5.5-SBD at higher [SBD—COO<sup>-</sup>]. This result may be interpreted to imply that the CAT16 aggregates assume more of a rodlike micellar shape, which allows a closer packing of the monomers in the aggregates. Structures **5** (1.5-SBD) and **5** (5.5-SBD) can accommodate such a characteristic but certainly cannot be said to be unique in this regard.

The correlation time results shown in Figure 5 reveal that the CAT16 monomer/SBD complexes bind more strongly as the [SBD-COO<sup>-</sup>] increases beyond 0.05 M for both the 1.5-SBD and 5.5-SBDs. This result is expected on the basis of the formation of structures such as **3**.

As mentioned above, the cause of the decrease in the fraction of aggregates is not obvious for the 5.5-SBD and requires explanation. One possibility, accepting structure 4 as a starting point, is that "dimers" or related structures for which the bilayer condensed on the SBD surface are formed (Scheme 3, 4 (5.5-SBD)). Another possibility is related to a constraint on supramolecular structures imposed by the actual size of the CAT16/SBD aggregates, effectively a *supramolecular steric effect*, which we now consider briefly.

Volume Considerations of the Supramolecular Assemblies Formed between Surfactants and SBDs. Supramolecular **Steric Effects**. Table 2 reports the volumes and occupancy of a 1 dm<sup>3</sup> solution calculated for different kinds of the largest molecular (1.5-SBD, 5.5-SBD) and supramolecular (5 (1.5-SBD), 5 (5.5-SBD)) "particles" that are postulated to be present in the CAT16 1.5- or 5.5-SBD at high [SBD-COO<sup>-</sup>]. For calculation of the particle volume occupancy several assumptions were made: (i) it has a spherical dynamic shape; (ii) the radius of the micelles corresponds to the length of the CAT16 molecule; (iii) the CAT16 adsorbed bilayer or monolayer only covers a portion of the dendrimer surface, so the particles were oblate and the occupancy volume was calculated by using as a diameter of a sphere the dimension of the dendrimer plus the dimension of the mono- or bilayer; (iv) a concentration of 0.5 mM in macromolecules (total [SBD-COO<sup>-</sup>] = 0.02 M) interacts with the aggregates of CAT16 ([CAT16] = 1 mM); (v) only a negligible fraction of CAT16 micelles do not interact with the dendrimers.

TABLE 2: Molecular Volumes and Percentage of Volume Occupancies of a 1 dm<sup>3</sup> Solution of CAT16 and SBD under Several Conditions<sup>a</sup>

	volume $(10^{-27} \text{ dm}^3)$	occupancy (%)			
Volume of "Particles"					
CAT16 micelle	$1.0 \times 10^{5}$	0.2			
1.5-SBD	$2.5 \times 10^{4}$	25			
5.5-SBD	$5.9 \times 10^{5}$	35			
Volume of Supramolecular Complexes early generation (1.5-SBD + CAT16))					
1.5-SBD + CAT16 bilayer	$4.7 \times 10^{5}$	14			
free 1.5-SBD	$2.5 \times 10^{4}$	24			
later generation $(5.5-SBD + CAT16)$					
5.5-SBD + CAT16 bilayer	$2.3 \times 10^{6}$	69			
free 5.5-SBD	$5.9 \times 10^{5}$	18			

<sup>a</sup> Length of a CAT16 monomer was assumed to be 25Å. Size of the 1.5-SBD was assumed to be 28 Å. Size of the 5.5-SBD was assumed to be 88 Å.

From Table 2 it is seen that the volume occupancy due to free SBD and to CAT16/SBD supramolecular structures is ca. 40% for the 1.5-SBD but ca. 90% for the 5.5-SBD. The conclusion from these computations is that at high [5.5-SBD], the formation of supramolecular assemblies such as 5 (5.5-SBD) may be inhibited by a "supramolecular steric effect", i.e., the number of "particles" such as 5 that can fit into a finite volume of solution limits their formation.

From these considerations, we postulate the formation of a small quantity of supramolecular structures (Scheme 3, 5) whereas most CAT16 remained as micelles. At higher dendrimer concentrations, the percentage of aggregates became almost invariant to further increases of [SBD–COO<sup>-</sup>], suggesting the major contribution of CAT16 micelles. The trend of  $\omega_{\rm ex}$  toward the value of CAT16 micelles (Figure 6) at high [SBD–COO<sup>-</sup>] is also consistent with this postulate.

Comparison of Fluorescence and EPR Probes of Surfactant—Dendrimer Supramolecular Assemblies. Finally, we need to reconcile the apparent discrepancy between the results of the EPR study reported here and a previous investigation <sup>17</sup> of *n*.5-SBD-induced aggregation of dodecyltrimethylammonium bromide (DTAB) by the pyrene fluorescence method (*vide supra*). For the latter system, it was found that the later the generation, the more efficient the SBD in inducing aggregation of DTAB. Conversely, from Table 1 it was found that the later generations are less effective in inducing aggregation. Although the surfactants (CAT16 and DTAB) possess different chain lengths and head groups, the apparent qualitative difference in behavior in induced aggregation is striking and requires clarification.

The results in Figure 3 show that in the presence of n.5-SBDs two types of static quenching occur, one at lower [CAT16] and a second at higher [CAT16]. At lower [CAT16] complexes such as  $\bf 3$  are prevalent, so therefore it is to be expected that the pyrene will be bound to sites near the hydrophobic CAT16 chain and be quenched statically. At higher [CAT16], supramolecular structures such as  $\bf 4$  are prevalent and the static quenching will be even more efficient because of the greater solubility of pyrene in the perturbed micelles and because of the high quenching efficiency due to the high concentration of the nitroxide groups in the aggregates.

Static quenching probably does not arise from the electrostatic interaction between the positively charged CAT16 head groups and the SBD-COO<sup>-</sup> groups, since the Stern-Volmer plot obtained using 4-trimethylammonium-2,2,6,6-tetramethylpiperidine-*N*-oxyl iodide (CAT1, which does not possess a hydrophobic chain) only showed dynamic quenching of pyrene,

implying unrestricted diffusional motion of the pyrene (results not shown). Furthermore, the Stern-Volmer plot for CAT1 was the same in the absence and presence of n.5-SBDs and corresponds to a bimolecular rate constant  $k_{\rm q}=6\times 10^9~{\rm M}^{-1}~{\rm s}^{-1}$ , a value expected for diffusion-controlled quenching.

Thus, the fluorescence-quenching results of Figure 3 are completely consistent with the model structures presented in Schemes 2 and 3. It appears that the apparent discrepancy between the EPR (Table 1) and fluorescence probes<sup>17</sup> in monitoring surfactant/SBD aggregates is simply related to the differences in concentration of SBD employed in the two studies and the unanticipated change in the supramolecular CAT16/ SBD structures occurring with a change in concentration (Scheme 3, 3 (1.5-SBD)  $\rightarrow$  4 (1.5-SBD) and 3 (5.5-SBD)  $\rightarrow$  4 (5.5-SBD)). For instance, the SBD concentration used for the experiments in Table 1 was much larger (0.2 M) than the concentration used for the fluorescence measurements (0.01 M for the DTAB system<sup>17</sup> and 5 mM for the fluorescencequenching measurements reported here). The 0.2 M concentration was used to offer a larger surface available to the interaction with the CAT16 aggregates and to guarantee a strong perturbation of the aggregation conditions.

Indeed, the data reported in Figure 4 support the conclusion that different [SBD] are responsible for the discrepancy in the EPR and fluorescence methods. Previous studies <sup>18-22,36</sup> have demonstrated the formation of complexes between polyelectrolytes and surfactants of opposite charges. These authors show that the electrostatic forces are reinforced by a cooperative process involving aggregation of the alkyl chains of the bound surfactant molecules. This is in line with the results obtained by using CAT16 surfactants binding the n.5-SBD surface. Furthermore, it has been claimed that the formation of a double layer of surfactant molecules at the polymer surface accounts for the solubilization of the complexes at high surfactant concentration. Since no precipitates were formed in the CAT16-n.5-SBD systems, this supports the hypothesis of bilayers of CAT16 at the SBD/water interface. Finally, the above authors indicated that the higher the density charge in the polyelectrolyte, the higher the cooperativity of the surfactants in the binding. This finding is in line with the larger aggregation of CAT16 at the surface of the high generation dendrimers. However, our results provide further insight of the polyelectrolyte-surfactant complexation by identifying various supramolecular structures as a function of the SBD concentration.

### Conclusion

An EPR investigation of a spin-labeled cationic surfactant, CAT16, has provided information on the supramolecular structures formed when the surfactant (above its cmc) is added at fixed concentration to a solution containing SBD. The structures produced depend on the SBD generation and on the SBD concentration. The EPR parameters percentage of signal f,  $\tau_c$ , and  $A_N$  report on the supramolecular structures involving complexes of surfactant monomers that are randomly and noncooperatively bound to the SBD surface (3, Scheme 2), and percentage of signal m and  $\omega_{\rm ex}$  report on the supramolecular structures involving surfactant monomers that are cooperatively aggregated into micelles (in the absence of SBD) or into micellelike aggegates bound to one or more SBD (4 and 5, Scheme 3). These parameters were investigated as a function of [CAT16], the addition of strong electrolytes, SBD generation, and [SBD] in order to obtain an extensive overview of the aggregation behavior of CAT16 in the absence and presence of SBD and to complement an earlier investigation<sup>8</sup> of the interactions of CAT surfactants below their cmc with SBD.

These conclusions obtained from the EPR measurements were supported by fluorescence-quenching investigations.

The proposed supramolecular structures in Schemes 2 and 3 allow a plausible and self-consistent interpretation of all the EPR results reported in the figures and the results of fluorescence probing of the structures formed between cationic surfactants and SBD.

In the absence of SBD above concentrations of ca. 0.5 mM, CAT16 forms micelles that were found by EPR to be in equilibrium with significant amounts of CAT16 monomers, even at relatively high [CAT16]. The ability to detect simultaneously an EPR signal of the monomer and the micelle allowed the simultaneous extraction of the EPR monomer and micellar parameters. At the typical [CAT16] of 1 mM employed in this investigation, about 60% of the CAT16 monomers existed in the micelle structure and were characterized by a spin exchange frequency,  $\omega_{\rm ex}$ , of  $6.2 \times 10^8 \, {\rm s}^{-1}$ . The monomers in equilibrium with the micelles were characterized by a  $\tau_{\rm c}$  of 27 ps and an  $A_N$  of 16.9 G.

In the presence of 1.5-SBD at 1 mM of CAT16, supramolecular structures between CAT16 and SBD were formed. At low concentration of SBD the structures are proposed to be (1) complexes of 1.5-SBD/CAT16 consisting of isolated CAT16 monomers ionically bound to the SBD (Scheme 2, 3) characterized by a  $\tau_c$  of 35 ps and an  $A_N$  of 16.9 G and (2) assemblies of perturbed CAT16 micelles and a single 1.5-SBD (Scheme 3, 4 (1.5-SBD)) characterized by  $\omega_{\rm ex}$  of 5.7  $\times$  10<sup>8</sup> s<sup>-1</sup> and a maximum fraction of ca. 80% at [SBD-COO<sup>-</sup>] of ca. 20 mM. At higher [SBD-COO<sup>-</sup>] the increased number of surface groups and number of SBD molecules available for binding (together with increasing ionic strength) first cause a redistribution of monomers to form a greater fraction of complexes 3 and then formation of higher order assemblies consisting of distorted micelles decorated by more than one 1.5-SBD (Scheme 3, 5). The value of  $\tau_c$  increases to a limiting value of 50 ps, and the value of  $A_N$  decreases to 16.6 G for 3, indicating a tighter binding and less polar environment for these complexes at higher [SBD-COO<sup>-</sup>]. The value of  $\omega_{\rm ex}$  increases to 6.6  $\times$  10<sup>8</sup> s<sup>-1</sup>, indicating a denser packing of CAT16 monomers for 5 relative to 4.

In the presence of 5.5-SBD at 1 mM of CAT16, supramolecular structures between CAT16 and SBD were also formed. At low concentration of SBD the structures are proposed to be (1) complexes of 5.5-SBD/CAT16 consisting of isolated CAT16 monomers bound to the SBD by both ionic and hydrophobic interactions (Scheme 2, 3) characterized by a  $\tau_c$  of 70 ps and an  $A_N$  of 16.5 G and (2) assemblies of distorted CAT16 micelles and a single 5.5-SBD (Scheme 3, 4 (5.5-SBD)) characterized by  $\omega_{\rm ex}$  of 5.1  $\times$  10<sup>8</sup> s<sup>-1</sup> and a maxima fraction of ca. 85% at [SBD-COO<sup>-</sup>] of ca. 20 mM. At higher [SBD-COO<sup>-</sup>] the increased number of surface groups and number of SBD molecules available for binding (together with increasing ionic strength) first cause a redistribution of monomers to form a greater fraction of complexes 3 and then formation of higher order assemblies consisting of two or more 5.5-SBD (Scheme 3, 5 (5.5-SBD)) together with a large fraction of CAT16 micelles. The reason for the onset of micelle formation is attributed to the large volume fraction (a supramolecular steric effect) required for the formation of assemblies such as 5 (5.5-SBD).

The EPR spin-labeled surfactant probe method has been shown to provide information on the supramolecular structures formed when SBD and surfactants above the cmc interact. These EPR results complement those reported earlier<sup>8</sup> for SBD and spin-labeled surfactants below the cmc and are consistent with studies of SBD and surfactants investigated by the fluorescence

method.<sup>17</sup> The structures deduced involving the noncovalent binding characteristic of supramolecular systems suggest a rich array of structural possibilities for producing novel aggregates between polyelectrolytes and SBD employing the principles of supramolecular chemistry. We hope the results will stimulate further experimentation in the design of supramolecular structures involving dendrimers and noncovalently associating species such as polyelectrolytes and water soluble polymers.

**Acknowledgment.** N.J.T. and S.J. thank the AFOSR and the NSF for their generous support. D.A.T. thanks the New Energy and Development Organization (NEDO) of the Ministry of International Trade and Industry of Japan (MITI) for their generous support and certain critical synthetic efforts. S.J. thanks the German Academic Exchange Service for support by a grant. M.F.O. thanks the Italian Ministero Università e Ricerca Scientifica e Tecnologica (MURST) and the Italian Consiglio Nazionale delle Ricerche (CNR) for financial support.

**Supporting Information Available:** A figure showing the variation of the surface tension (dyn/cm) as a function of —log [CAT16] to evaluate the cmc of CAT16 (1 page). Ordering information is given on any current masthead page.

# **References and Notes**

- (1) (a) Tomalia, D. A.; Baker, H.; Dewald, J; Hall, M.; Kallos, G.; Martin, S.; Roeck, J.; Smith, P. Polym. J. (Tokyo) 1985, 17, 117. (b) Tomalia, D. A.; Baker, H.; Dewald, J; Hall, M.; Kallos, G.; Martin, S.; Roeck, J.; Smith, P. Macromolecules 1986, 19, 2466. (c) Tomalia, D. A.; Berry, V.; Hall, M.; Hedstrand, D. M. Macromolecules 1987, 20, 1164. (d) Tomalia, D. A.; Hall, M.; Hedstrand, D. M. J. Am. Chem. Soc. 1987, 109, 1601. (e) Padias, A. B.; Hall, H. K.; Tomalia, D. A.; McConnell, J. R. J. Org. Chem. 1987, 52, 5305. (f) Wilson, L. R.; Tomalia, D. A. Polym. Prepr. (Am. Chem. Soc., Div. Polym. Chem.) 1989, 30, 115. (g) Padias, A. B.; Hall, H. K.; Tomalia, D. A.; Polym. Prepr. (Am. Chem. Soc., Div. Polym. Chem.) 1989, 30, 119. (h) Meltzer, A. D.; Tirell, D. A.; Jones, A. A.; Inglefield, P. T.; Downing, D. M. Tomalia, D. A. Polym. Prepr. (Am. Chem. Soc., Div. Polym. Chem.) 1989, 30, 121. (i) Tomalia, D. A.; Naylor, A. M.; Goddard, W. A., III Angew Chem., Int. Ed. Engl. 1990, 29, 138. (j) Tomalia, D. A.; Dewald, J. R. U.S. Patent 4 507 466, 1985. Tomalia, D. A.; Dewald, J. R. U.S. Patent 4 558 120, 1985. Tomalia, D. A.; Dewald, J. R. U.S. Patent 4,568,737, 1986. Tomalia, D. A.; Dewald, J. R. U.S. Patent 4,587,329, 1986. Tomalia, D. A.; Dewald, J. R. U.S. Patent 4,631,337, 1986. Tomalia, D. A.; Dewald, J. R. U.S. Patent 4,694,064, 1986. Tomalia, D. A.; Dewald, J. R. U.S. Patent 4,857,599, 1989.
- (2) Advances in Dendritic Macromolecules; Newkome, G. R., Ed.; JAI Press: Greenwich, CT, 1993.
- (3) (a) Krohn, K. Starburst Dendrimers and Arborols. *Org. Synth. Highlights* 1991, 378. (b) Amato, L. Trekking in the Molecular Forest. *Sci. News* 1990, *138*, 298. (c) Newkome, G. R.; Moorefield, C. N.; Baker, G. R.; Johnson, A. L.; Behera, R. K. *Angew. Chem., Int. Ed. Engl.* 1991, *30*, 1176. (d) Newkome, G. R.; Moorefield, C. N.; Baker, G. R.; Saunders, M. J.; Grossman, S. H. *Angew. Chem., Int. Ed. Engl.* 1991, *30*, 1178. (e) Kim, Y. H.; Webster, O. W. *J. Am. Chem. Soc.* 1990, *112*, 4592. (f) Hawker, C. J.; Wooley, K. L.; Fréchet, J. M. J. *J. Chem. Soc., Perkin Trans.* 1 1993, 1287. (g) Newkome, G. R.; Young, J. K.; Baker, G. R.; Potter, R. L.; Audoly, L.; Cooper, D.; Weis, C. D. *Macromolecules* 1993, *26*, 2394.
- (4) Naylor, A. M.; Goddard, W. A., III; Kiefer, G. E.; Tomalia, D. A. J. Am. Chem. Soc. **1989**, 111, 2341.
- (5) Moreno-Bondi, M. C.; Orellana, G.; Turro, N. J.; Tomalia, D. A *Macromolecules* **1990**, 23, 910.
- (6) Gopidas, K. R.; Leheny, A. R.; Caminati, G.; Turro, N. J.; Tomalia, D. A. J. Am. Chem. Soc. 1991, 113, 7335.
- (7) Ottaviani, M. F.; Bossmann, S.; Turro, N. J.; Tomalia, D. A. J. Am. Chem. Soc. **1994**, 116, 661.
- (8) Ottaviani, M. F.; Cossu, E.; Turro, N. J.; Tomalia, D. A. J. Am. Chem. Soc. 1995, 117, 4387.
- (9) (a) Spin Labeling. Theory and Applications; Berliner, L. J. Ed.; Academic Press: New York, 1976; Vol. 1; 1979, Vol. 2. (b) Biological Magnetic Resonance. Spin Labeling. Theory and Applications; Berliner, L. J., Reuben, J., Eds.; Plenum Press: New York, 1989; Vol. 8.
- (10) Taupin, C.; Dvolaitoky, M. In *Surfactant Solutions. New Methods of Investigation*; Zana, R., Ed.; Surfactant Science Series, 22; Marcel Dekker: New York, 1987; p 359.
  - (11) Hearing, G.; Luisi, P. L.; Hauser, H. J. Phys. Chem. 1983, 92, 3574.
  - (12) Yoshioka, H.; Kazama, S. J. Colloid Interface Sci. 1983, 95, 240.
  - (13) Wikander, G.; Johansson, L. B.-A. Langmuir 1989, 5, 728.

- (14) (a) Baglioni, P.; Ferroni, E.; Martini, G.; Ottaviani, M. F. *J. Phys. Chem.* **1984**, *88*, 5187. (b) Baglioni, P.; Ottaviani, M. F.; Martini, G. *J. Phys. Chem.* **1986**, *90*, 5878.
- (15) (a) Bales, B. L.; Kevan, L. J. Phys. Chem. **1982**, 86, 3836. (b) Bratt, J. P.; Kevan, L. J. Phys. Chem. **1992**, 96, 6849. Bratt, J. P.; Kevan, L. J. Phys. Chem. **1993**, 96, 6849.
- (16) (a) Bonosi, F.; Gabrielli, G.; Margheri, E.; Martini, G. *Langmuir* **1990**, *6*, 1769. (b) Ristori, S.; Ottaviani, M. F.; Lenti, D.; Martini, G. *Langmuir* **1991**, *7*, 1958. (c) Ristori, S.; Martini, G. *Langmuir* **1992**, *8*, 1937. (d) Martini, G.; Ottaviani, M. F.; Ristori, S. *Croat. Chim. Acta* **1992**, *65*, 471.
- (17) Caminati, G.; Turro, N. J.; Tomalia, D. A. J. Am. Chem. Soc. 1990, 112, 8515.
- (18) Goddard, E. D. Colloids Surf. 1986, 19, 255. Goddard, E. D. Colloids Surf. 1986, 19, 301.
- (19) Robb, I. D. In *Anionic Surfactants: Physical Chemistry of Surfactant Actions*; Lucassen-Reynders, E. H., Ed.; Marcel Dekker: New York, 1981; p 109.
- (20) Goddard, E. D.; Hannan, K. B. In *Micellization, Solubilization and Microemulsions*; Mittal, K. L., Ed.; Plenum Press: New York, 1977; Vol. 2.
- (21) Brackman, J. C.; Engberts, J. B. F. N. Chem. Soc. Rev. 1993, 85.
- (22) Gao, Z.; Kwak, J. C. T.; Labonte, R.; Marangoni, G.; Wasylishen, R. E. Colloids Surf. 1990, 45, 269.
- (23) Blackmore, E. S.; Tiddy, G. J. T. *J. Chem. Soc., Faraday Trans.* 2 **1988**, *84*, 1115.
- (24) (a) Kivelson, D. J. Chem. Phys. 1957, 27, 1087. (b) Plachy, W.; Kivelson, D. J. Chem. Phys. 1967, 47, 3312.

- (25) Sackmann, E.; Träuble, T. J. Am. Chem. Soc. 1972, 94, 4482, 4492, 4499
- (26) Aizawa, M.; Komatsu, T.; Nakagawa, T Bull. Chem. Soc. Jpn. 1979, 52, 980. Aizawa, M.; Komatsu, T.; Nakagawa, T Bull. Chem. Soc. Jpn. 1980, 53, 975.
- (27) Schneider, D. J.; Freed, J. H. In *Biological Magnetic Resonance*. *Spin Labeling. Theory and Applications*; Berliner, L. J., Reuben, J., Eds.; Plenum Press: New York, 1989; Vol. 8, p 1.
- (28) (a) Janzen, E. G. *Top. Stereochem.* **1971**, *6*, 117. (b) Ottaviani, M. F.; Martini, G.; Nuti, L. *Magn. Reson. Chem.* **1987**, 25, 897.
- (29) Atik, S. S.; Kwan, C. L.; Singer, L. A. J. Am. Chem. Soc. 1979, 101, 5696.
- (30) (a) Wennerström, H.; Lindman, B. *Phys. Rep.* **1979**, *52*, 1–89. (b) Lindman, B.; Wennerström, H. *Top. Curr. Chem.* **1980**, *87*, 1–80.
- (31) Rosen, M. J. Surfactants and Interfacial Phenomena; Wiley: New York, 1978.
- (32) (a) Kalyanasudaram, K. *Photophysics of Microheterogeneous Systems*; Academic Press: New York, 1988. (b) Thomas, J. K. *The Chemistry of Excitation at Interfaces*; ACS Monograph; American Chemical Society: Washington, DC, 1984.
- (33) Kalyanasudaram, K.; Thomas, J. K. J. Am. Chem. Soc. 1977, 99, 2039
- (34) Aizawa, M.; Komatsu, T.; Nakagawa, T. Bull. Chem. Soc. Jpn. 1980, 53, 975.
  - (35) Lehn, J.-M. Supramolecular Chemistry; VCH: New York, 1995.
  - (36) Wasserman, A. M. Russ. Chem. Rev. 1994, 63, 373.

JP960291R